

Research Article

Open Access

Stefano Gaggero, Tomaso Gaggero*, Enrico Rizzuto, Giorgio Tani, Diego Villa, and Michele Viviani

Ship propeller side effects: pressure pulses and radiated noise

DOI 10.1515/noise-2016-0021

Received Jun 27, 2016; accepted Dec 12, 2016

Abstract: The present paper deals with the side effects of propellers cavitation, *i.e.* pressure pulses and radiated noise. These effects are gaining more and more importance for commercial ships for different reasons. Pressure pulses significantly affect comfort onboard, thus their reduction is of utmost importance for all ships carrying passengers. As regards the underwater radiated noise, in the last decade interest has shifted from navy applications to commercial ships, due to the concern for the rising background noise in the oceans. The propellers, generating noise directly in water, represent one of the main contributions to the overall underwater noise emitted from ships. Due to the complexity of the mechanisms of propeller noise generation, different complementary strategies have to be followed to properly analyze the problem, ranging from induced pressure pulses to broadband noise and cavitation. In the present work, part of the activities carried out in the framework of the collaborative EU FP7 project AQUO (Achieve QUIeter Oceans by shipping noise footprint reduction, www.aquo.eu) are reported.

The paper presents the investigations carried out on a specific test case represented by a single screw research vessel, which is analyzed with three different strategies: numerical calculations, model scale investigations and full-scale measurements.


Keywords: ship underwater noise; propeller side effects; cavitation noise; pressure pulses; AQUO Project

***Corresponding Author: Tomaso Gaggero:** DITEN – Department of Naval, Electrical, Electronic and Telecommunication Engineering, University of Genova, Polo Marconi, La Spezia, Italy; Email: tomaso.gaggero@unige.it

Stefano Gaggero, Giorgio Tani, Michele Viviani: DITEN – Department of Naval, Electrical, Electronic and Telecommunication Engineering, University of Genova, Genova, Italy

Enrico Rizzuto: DII – Department of Industrial Engineering University of Naples Frederick II, Napoli, Italy

Diego Villa: DITEN – Department of Naval, Electrical, Electronic and Telecommunication Engineering, University of Genova, Polo Marconi, La Spezia, Italy

 © 2016 S. Gaggero *et al.*, published by De Gruyter Open. This work is licensed under the Creative Commons Attribution-NonCommercial-NoDerivs 3.0 License.

1 Introduction

The design of marine propellers has considerably evolved during time, due to the introduction of more demanding requirements and the parallel development of more accurate design and analysis procedures. Design requirements are no more limited to the “classical” search for high efficiency and erosive cavitation avoidance, but include, at least for the “high added value ships” (passenger ships, mega yachts, oceanographic ships, naval ships, etc.) stringent requirements in terms of pressure pulses and radiated noise.

The problem of pressures pulses is of great importance when high level of comfort onboard are requested. This is obviously a stringent requirement for passenger ships and yachts, for which very low levels of accelerations are admitted, leading, therefore, to the necessity of very low pressure pulses. The prediction of pressure pulses has been treated for long time in the context of marine propellers design, both experimentally and numerically. Various methods to approach this problem have been proposed during years by different authors, ranging from potential flow solvers (lifting surface and panel codes) to more accurate and time demanding viscous codes (RANSE solvers). The application of these numerical approaches leads, of course, to different levels of accuracy and complexity, which depends also on the functioning point considered (*e.g.* design pitch or reduced pitch for CPP, cavitation extent, etc.). Also from the experimental point of view, different approaches may be utilised, mainly depending on the facility capabilities (*e.g.* use of complete ship models in case of larger facilities such as large cavitation tunnels, circulating water channels or depressurised towing tank, wake screens or similar equipment in case of smaller facilities). In all cases, anyway, one of the most significant issues is probably represented by the correct prediction and representation of the full-scale wake, which obviously affects the experimental result and, in turn, the full scale prediction.

The problem of propeller radiated noise has been related for many years almost only to naval ships require-

ments. Only recently, the concern about the effects that underwater noise emissions may have on the marine fauna and particularly on marine mammals has increased.

Marine mammals heavily depend on sound to communicate, to orient themselves and to find food and mates. Anthropogenic noise can have different effects on the cetaceans, ranging from hearing permanent or temporal injuries to behavioural changes and communication masking. The latter aspect, in particular, seems to be directly correlated to the increase in the last decades of the diffused background noise in the oceans due to the parallel increase of the world-spread shipping traffic.

From a formal point of view, this subject is to be covered by MARPOL, as energy emissions have been included among the various forms of possible noxious emissions [1]. This aspect has not been yet regulated, but it has come to the attention of the Marine Environmental Pollution Committee (MEPC) of IMO [2] and of other Regulatory bodies, like the National Oceanic and Atmospheric Administration (NOAA) and the European Union Commission.

The EU, in particular, has funded in the last decade different research projects aimed to this study (SILENV [3], SONIC [4] and AQUO [5]). In particular, the AQUO project was aimed at providing the Regulator with a tool able to assess and manage the environmental impact due to the presence of a given number of ships on a particular marine area, considering in particular cavitating propeller noise. In the project, therefore, attention has been given to the various methods for the prediction of propeller radiated noise; parallel activities have been moreover devoted to the prediction of pressure pulses. In the present work, the numerical and the experimental activities carried out by UNIGE in the framework of the AQUO project for both the aims are presented and calculations are, then, validated against full-scale results.

For what regards pressure pulses, the numerical activities have been aimed to the development and validation of a set of numerical tools capable of predicting the self-propulsion point at first and, then, to provide the related pressure pulses on the hull. One of the aims of the activity was to analyse and employ numerical approaches not too computationally expensive. The prediction of the self-propulsion point has been carried out by means of a coupled BEM/RANSE approach (firstly introduced by [6] and developed also in [7]) while the pressure pulses have been predicted by means of only the BEM code [8]. The numerical results have been compared with the model scale measurements at the cavitation tunnel of the University of Genoa and with the full-scale observations. The first comparison provides a useful validation of the numerical computations in a case study more controlled than the real pro-

peller operating in full scale, as the case of the sea trials measurements. Moreover, the comparison between model and full-scale results provides an insight into the problem of pressure pulses prediction by means of model scale tests.

For what concerns radiated noise, its prediction (especially when dealing with broadband noise) is far beyond the possibilities of the numerical approaches adopted for pressure pulses computations. This, in principle, would require a much more demanding computational approach, as LES, DES or other more complex methods, with the requirement for much finer meshes, much higher computational power and time. Even if in the context of the AQUO project some efforts have been devoted to these predictions [9, 11], the University of Genoa was not directly involved in these activities, which are thus not presented in the present work. The focus, consequently, is pointed to the model scale tests and to their comparison to full-scale measurements, among those addressed in the AQUO project, in the case of a single screw research vessel, described in section 2. The numerical and experimental activities (in both model and full-scale) are presented in sections 3 and 4 respectively. Finally, in section 5, a summary of the numerical and experimental results in terms of both pressure pulses and radiated noise is presented.

2 Case study

The case study is represented by the Navigator XXI research vessel [12]. The main dimensions of the ship are reported in Table 1. The ship is equipped with a single controllable pitch propeller (Figure 1), whose main dimensions are summarized in Table 2, moved by a seven cylinder 4 stroke diesel engine.



Figure 1: The RV Navigator XXI controllable pitch propeller.

Table 1: Main dimensions in full scale of the RV Navigator XXI.

<i>Data</i>	<i>Symbol</i>	<i>Full scale dimensions (scale factor $\lambda = 10$)</i>
Length overall	L_{OA} [m]	60.30
Length on waterline	L_{WL} [m]	55.16
Length between perpendiculars	L_{BP} [m]	54.13
Breadth moulded	B [m]	10.50
Draught: fore – aft	T [m]	3.15 - 3.20
Depth	D [m]	4.20
Displacement volume	Δ [m ³]	1126
Wetted surface	WS [m ²]	672
Block coefficient	C_B [-]	0.623
Midsection coefficient	C_M [-]	0.915
Prismatic coefficient	C_P [-]	0.680
Waterline coefficient	C_W [-]	0.824

Table 2: Main dimensions in full scale of the RV Navigator XXI controllable pitch propeller.

<i>Data</i>	<i>Symbol</i>	<i>Full scale dimensions (scale factor $\lambda = 10$)</i>
Scale	λ [-]	-
Propeller Diameter	D [m]	2.26
Hub Diameter	D_H [m]	0.71
Number of blades	Z [-]	4
Skew (at tip)	SK [°]	22.5
Pitch Ratio at 0.7 r/R	P/D [-]	0.942

3 Numerical activities

In the framework of the AQUO project, the numerical activities carried out by the University of Genoa have been devoted to the development and validation of computationally affordable tools for the numerical prediction of propeller pressure pulses. These tools cover the ship wake and self-propulsion point prediction and the consequent pressure pulses induced on the stern of the hull. In general, from a numerical point of view, the application of LES or DES codes would be needed in order to properly evaluate the propeller inflow field, with a detailed characterization of the mutual interactions between the hull and the propeller itself. This is mandatory if attention is devoted to propeller radiated noise but it could be important also for a more accurate prediction of the pressure pulses, especially in off design conditions. Unfortunately, the complete

solution (hull and propeller together) by means of these codes would require prohibitive computational time and resources, not in line with the initial aim. A possible alternative in order to reduce the computational requests is represented by the use of a full RANSE approach (modeling both hull and propellers). This solution, even if faster, is still mainly confined to research activities because of the still too high demands for a day-by-day design activity, especially if interest is posed on cavitating conditions.

A viable alternative in order to save time and still have a reasonable accuracy at least in correspondence to the design point is the adoption of even simplified methods like those that have been proposed recently [13, 14] and that have been adopted in the AQUO project. A computationally efficient Boundary Element Method (BEM) code was used to predict the propeller performance, while a RANSE code was employed to evaluate the inflow field to the propeller. The coupling of the two codes was achieved by means of a body force approach. By using this approach, the propeller self-propulsion point is evaluated together with the nominal wake (hull wake in correspondence to the propeller disk in a pure towing test) and the effective wake (hull wake in front of the propeller considering their mutual interaction). Pressure pulses are, finally, evaluated a posteriori by means of dedicated BEM calculations with the inflow and the functioning point (propeller RPM) obtained by the self-propulsion prediction. The propeller non stationary functioning in cavitating conditions and the resultant pressure pulses may be consequently computed in a reasonable time and with sufficient accuracy, at least when the extension of the cavitation bubble is not too high, as discussed in the following.

The developed potential code adopted for the prediction of pressure pulses is able to solve the inviscid steady (and unsteady, in the case of a non-uniform velocity input) flow around a propeller by means of the *key blade* approach [15]. The influence of cavitation is considered by means of a quasi-nonlinear approach [16], which solves the sheet cavitating bubble adding proper sources (or sinks) on the blade surface to simulate the cavitation bubble thickness. Once the propeller is solved by imposing appropriate boundary conditions, it is straightforward to evaluate the velocity field in any point of the computational domain and, via the unsteady formulation of the Bernoulli theorem, derives the unsteady pressure distribution on the surfaces of interest (the hull stern or the flat plate adopted during cavitation tunnel tests). The solution is calculated, following the guidelines developed and extensively tested in previous works [17–19], by using about 1250 hyperbolical panels on the key blade and 1600 panels to model the hull stern or the flat plate. A detailed descrip-

Table 3: Wake configurations analysed.

<i>Inflow wake</i>	<i>Measurement Surface</i>	<i>Reference Experiment</i>
Nominal	Flat plate	UNIGE
Nominal - LDV	Flat plate	cavitation tunnel
Effective	Flat plate	tunnel
Nominal	Hull stern	Full scale
Effective	Hull stern	test

tion of the coupling procedure and of the developed BEM may be found in [8, 14].

In the present paper, as reported in Table 3, different inflow wakes have been considered in order to evaluate their influence on the pressure pulses prediction. Pressures have been computed, moreover, on two different surfaces (hull stern or flat plate), to compare them with the available experimental measurements; as described in Section 4, indeed, in model scale tests the hull was substituted by a flat plate reproducing only the correct propeller-hull clearance, while full scale tests obviously are referred to the real hull form.

For what regards the inflow wakes, both the full-scale nominal and effective wake, numerically evaluated with the coupled BEM/RANSE approach, have been considered and pressures have been calculated with the model tests configuration (flat plate) and with the full-scale configuration (stern hull form) in both cases.

In addition, the measured wake (Nominal – LDV) at the cavitation tunnel again with the flat plate configuration was also considered. Such wake presents obviously some differences with respect to the predicted RANSE full-scale nominal wake due to the adoption of wake screens. Nevertheless, it is interesting to consider the Nominal – LDV wake in order to have an insight into the possible influence of the approximated experimental reproduction by means of wire screens of a given wake.

4 Experimental activities

An extensive experimental campaign has been carried out for the case study presented in this work. Measurements focused on propeller cavitation, pressure pulses and noise both in full scale (sea trials) and model scale (experiments at cavitation tunnel).

This large experimental investigation allowed collecting a very useful set of data for the study of propeller cavitation and its side effects, gaining a better understand-

ing of such phenomena. Furthermore, both full scale and model scale results are valuable for the validation of numerical tools such as the ones previously described for the prediction of induced pressures or other tools for the prediction of radiated noise, not considered in present study. Finally, the comparison between model scale results and sea trials allows also to enhance and validate full-scale prediction procedures based on cavitation tunnel experiments, with particular attention on small scale facilities.

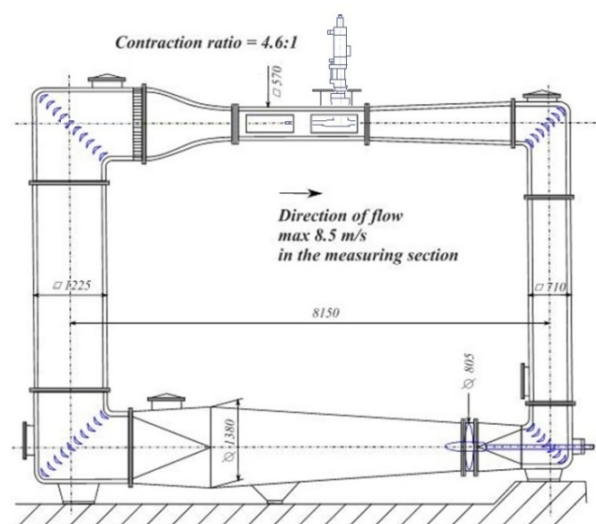
Actually, as far as radiated noise is concerned, model scale measurements still represent the most used and reliable tool for a full-scale prediction. Nevertheless, model tests present considerable issues (scale effects both on ship wake and on cavitation or confined environment effects for instance) which are still under discussion in the ITTC community [20].

The sea trials and the model scale experiments that were analyzed and that served for the validation of the numerical tools are described in the following subsections.

4.1 Cavitation tunnel measurements set-up and procedure

Model tests have been carried out at the cavitation tunnel of the University of Genova.

The facility is a Kempf & Remmers closed water circuit tunnel, featuring a squared testing section of 0.57 m × 0.57 m, with a total length of 2 m. The tunnel (shown schematically in Figure 2) is equipped with a Kempf &

**Figure 2:** The cavitation tunnel at the University of Genova.

Remmers H39 dynamometer, which measures propeller thrust, torque and RPM.

The importance of water quality for cavitation tests has been largely addressed by ITTC [21]. According to this, the oxygen content is constantly monitored by means of ABB dissolved oxygen sensor model 8012/170, coupled to an ABB analyzer AX400. Present tests were performed maintaining an oxygen content equal to about 40% of saturation value at atmospheric pressure.

As recommended by ITTC [22], in order to achieve realistic cavitation on the propeller the full-scale nominal wake field has to be considered during cavitation tests. In present work, as anticipated in Section 3, the nominal full-scale wake evaluated by means of RANSE calculations was assumed as the target wake to be modeled inside the cavitation tunnel.

Depending on the dimension of the facility, different techniques may be adopted to reproduce a given wake. In the present case the size of the test section prevents the adoption of a hull model, thus the propeller flow was simulated by means of wire screens placed upstream of the propeller, as shown in Figure 3. The screens have been built with a trial and error procedure, iteratively checking the obtained wake field by means of LDV measurements.

It has to be remarked that wire screens allow simulating only the axial wake field on the propeller. Usually the tangential components mainly consists in a vertical flow which is reproduced at the cavitation tunnel by an appropriate propeller shaft inclination. In present case, a different approach was adopted. The effect of the tangential flow on the blades, in terms of change of the angle of attack of the profiles, was computed and an equivalent axial wake disturbance was defined in order to reproduce the same angle of attack variations during a propeller revolution. This fictitious wake was then superimposed to the pure axial component of the nominal wake field predicted by RANSE, obtaining the final wake that has been then modeled at the cavitation tunnel. The final measured wake (in the following referred to as “Nominal – LDV”) is shown in Figure 4. A comparison with the target numerical wake is reported in section 5.

Cavitation tests, as usual, included the measurement of the inception index for all the different cavitation typologies occurring on the propeller. Cavitation observations, moreover, were carried out both visually and by means of three Allied Vision Tech Marlin F145B2 Firewire Cameras, with a resolution of 1392×1040 pixels and a frame rate up to 10 fps.

The experimental setup was completed by the presence of some further elements, adopted for the measurement of pressure pulses and radiated noise. In particular,

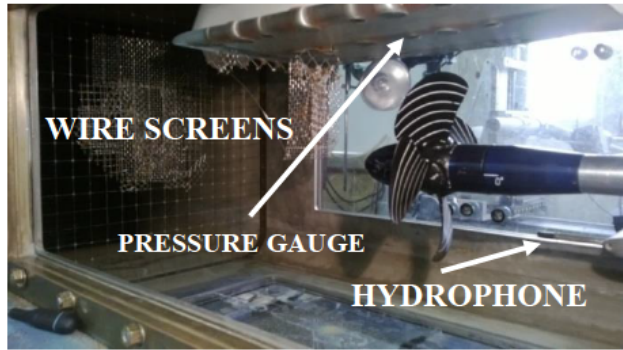


Figure 3: Experimental set-up within the UNIGE cavitation tunnel.

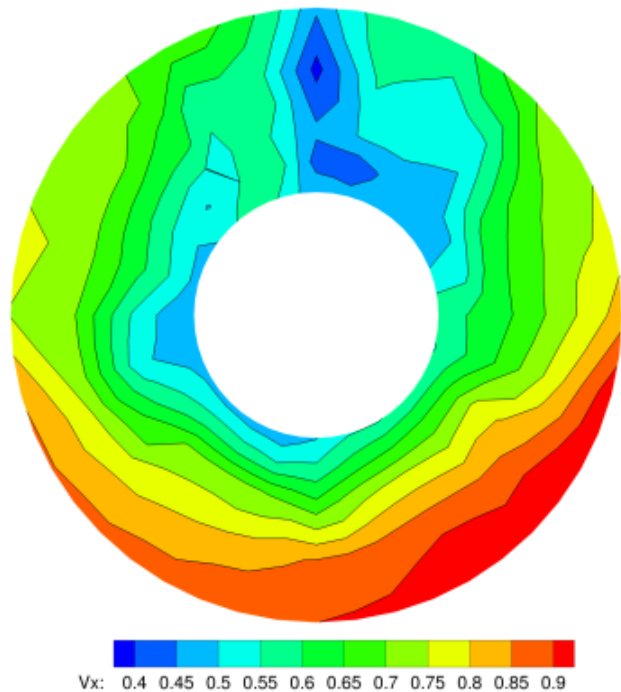


Figure 4: Target wake (left) and obtained wake (right) for cavitation tunnel tests.

a flat plate with faired leading and trailing edge was positioned above the propeller. This element, which houses the differential pressure sensor (EPX) adopted for pressure pulse measurements, should replicate the effect of the presence of the aft part of the ship above the propeller.

The distance between the flat plate and the propeller was adjusted in order to match the real clearance existing between the propeller and the hull of the ship. The sensor was positioned directly above the center of propeller disk.

Finally, two different hydrophones were adopted for noise measurements: a Reson hydrophone TC4013 and a Bruel and Kjaer 8103 hydrophone, together with the Bruel

side and starboard side (Figure 8). Three different hydrophones has been used at 5, 10 and 15 meters depth. Aim of deploying more than one hydrophone in the water column is to try to mitigate, averaging the three signals, the effects due to the possible vertical directivity of the source and due to the Lloyd's mirror effect. Similarly, the time at which data start to be recorded ("Start data") is important for the characterization of the source directivity in the horizontal plane [28]. As a matter of fact, the time duration of records (performed symmetrically around the closest point of approach "CPA") influences the range of variation of the angle formed between the buoy-ship line and the course of the ship. The longer the time record is, the wider is the range of angles, thus including data in a larger number of different reciprocal positions between the hull and the hydrophones during the ship advance. As shown in Figure 13, in [27] the amplitude of the relative horizontal angle is fixed at 60° (30° towards bow and 30° towards stern). Such angle identifies the segment of the recorded signal for which the spectra are evaluated. The minimum lateral distance the ship needs to keep from the hydrophone array is a function of the ship dimensions.

In the present case, the lateral distance was greater than a hundred meters. The variability of the distance implies a variability in the recorded levels at the hydrophone as propagation losses from the ship to the transducer depend, primarily, on the distance. It is therefore of paramount importance to refer the measurements to a standard distance from the source in order to allow comparison between different records. The standard in [27] suggests to normalise the sound levels to 1 meter from the source using the typical spherical law: $20\log(r)$. Such method is widely used and universally recognised, but sound propagation at sea is very complex and propagation losses may differ significantly from the spherical law, especially in low water depths, as discussed later.

The recorded signals were then post-processed in order to obtain spectrograms, $1/3$ octaves band spectra and the power spectral density functions. Data that will be shown in the next chapters are post processed following the procedure described in [29].

5 Results

A collection of the results of the propeller side effects (pressure pulses and radiated noise) is reported in this section. Only one working condition (the ship at its design load with a speed of 12 knots and the propeller at design pitch) has been chosen (and analyzed) as test case.

5.1 Pressure pulses

The pressure pulses have been predicted, as summarized in Table 3, by means of numerical calculations with different configurations in terms of propeller wake inflow and measurement surfaces. In order to have a better insight into the results, indeed, it is important to carry out pressure pulses predictions with the different wakes considered, together with the possible combinations of surfaces where pressures are evaluated. The nominal and the effective wake (both from numerical calculations in full-scale) are reported in Figure 7. As it can be seen, a rather marked difference exists between the two: in the case of the effective wake, the two bilge vortices are reduced in extension and shifted towards the propeller disk centre, where a more marked deceleration is present. At twelve o'clock position, a more marked decelerated area exists. The wake fraction of the effective wake, in addition, results slightly higher than in the case of the nominal wake (*i.e.* the effective wake is slower than the nominal).

The first difference may be ascribed to the interaction between the propeller and the hull, which tends to shift, towards the centre of the propeller disk, the more decelerated area near the hull. The second difference may be ascribed to different issues.

A slight overestimation of the propeller induced velocities by BEM in front of the propeller exists; this, due to the coupling procedure adopted, results into a slower effective wake. In addition to this, the effective wake should be evaluated in correspondence to the propeller disk. This may be achieved through extrapolation, due to the physical presence of the propeller or of equivalent body forces. As it is well known, the wake field upstream the propeller accelerates while approaching the propeller: as shown in [30] if this acceleration is not negligible, the location chosen for the effective wake evaluation may affect significantly the results. In particular, if the wake is not extrapolated at the propeller plane, it would result slower. This, in turn, could obviously affect propeller performance and cavitation. In order to reduce these discrepancies, in present calculations propeller analyses were carried out with the thrust identity assumption. By slightly adjusting the advance coefficient (changing the undisturbed inflow velocity), predictions of cavitation and pressure pulses were carried out with the propeller delivering an average unsteady thrust equal to that measured (or evaluated) during model and full scale tests. The effective wake obtained through the RANS/BEM coupling, consequently, serves only as a way to distribute the non-uniform velocity field on the propeller disk in a different way with respect to the nominal wake distribution that neglects the influence of the propeller.

Anyway, further analyses, as those proposed in [31] will be carried out in near future in order to further analyze this issue.

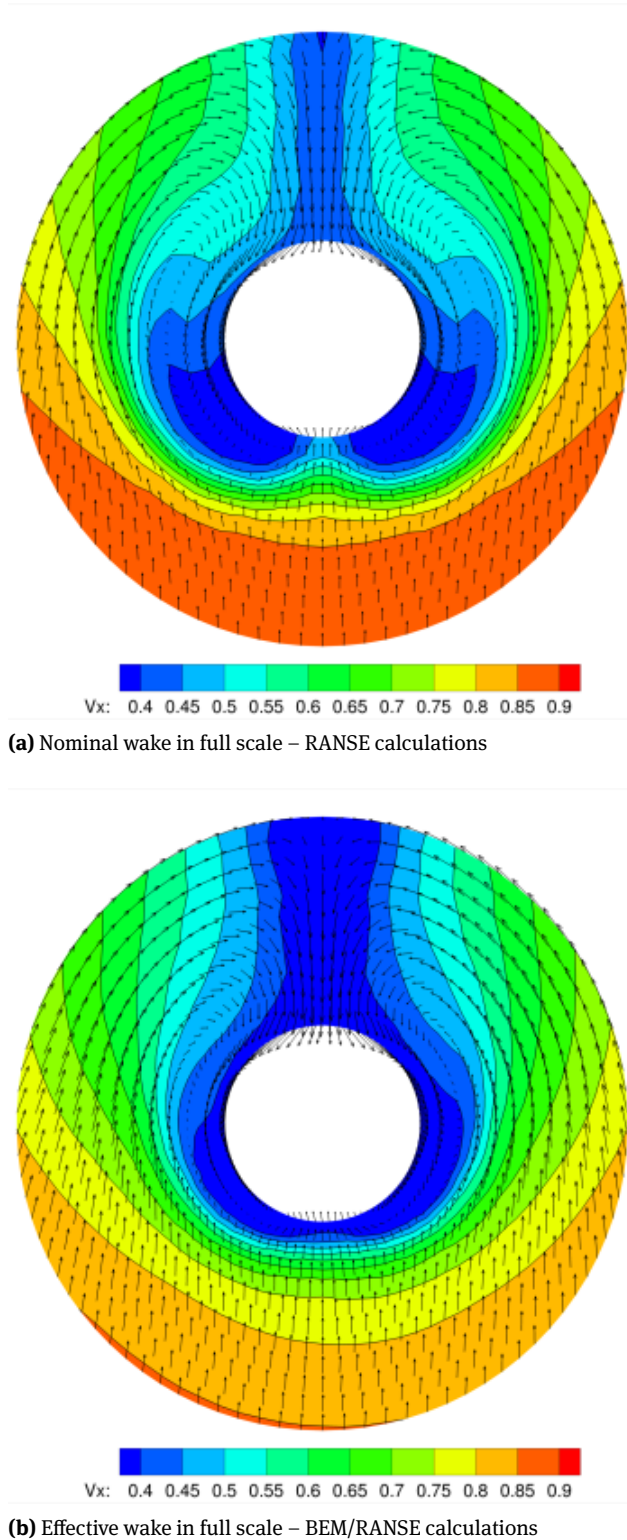


Figure 7: Nominal and Effective wakes in full scale

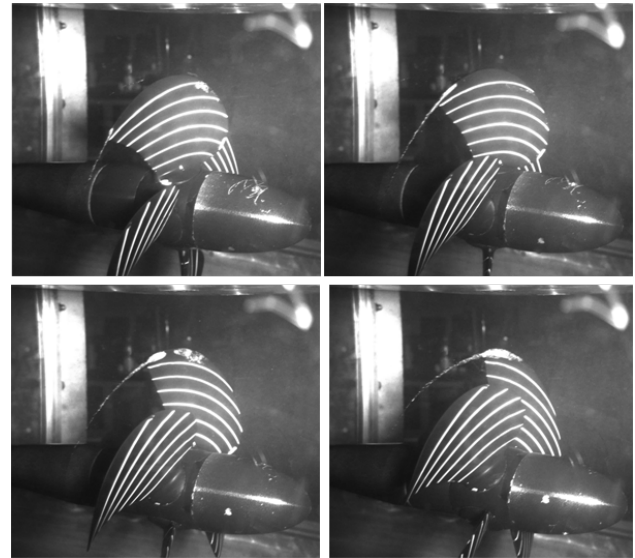


Figure 8: Observed cavity extension in UNIGE cavitation tunnel.

The nominal wake reproduced at cavitation tunnel (the Nominal – LDV wake shown in Figure 4) is different from the pure Nominal wake of Figure 7, since an equivalent axial wake was defined in order to account for the effect of the tangential velocities. Moreover, a further difference is induced by the experimental setup adopted (wake screen, propeller cap) which allows to reproduce only partially the target wake. The main differences are confined in the area close to the hub, which is the most complex to be modeled, because of the effect of the propeller cap, which results in a local flow acceleration, preventing the reproduction of the decelerated flow field at lower radiuses.

However, this part of the wake field has a weaker influence on propeller functioning, especially at the working condition considered in the present analysis. On the contrary, at the more important outer radii the agreement between the two wakes is acceptable. Exactly in order to have an insight into the influence of these discrepancies calculations have been repeated with the model scale configuration (flat plate above the propeller) using both the Nominal full scale numerical wake and Nominal – LDV measured wake at the cavitation tunnel.

Before moving to pressure calculations, the predicted cavitation extent in correspondence to the three hull wakes under investigation has been compared with the experimental observations at the cavitation tunnel in the same condition.

This analysis allows having a better understanding of the pressure pulses results. As it can be seen from the results reported in Figure 8 and Figure 9, a very good correspondence of sheet cavitation extent (in both radial

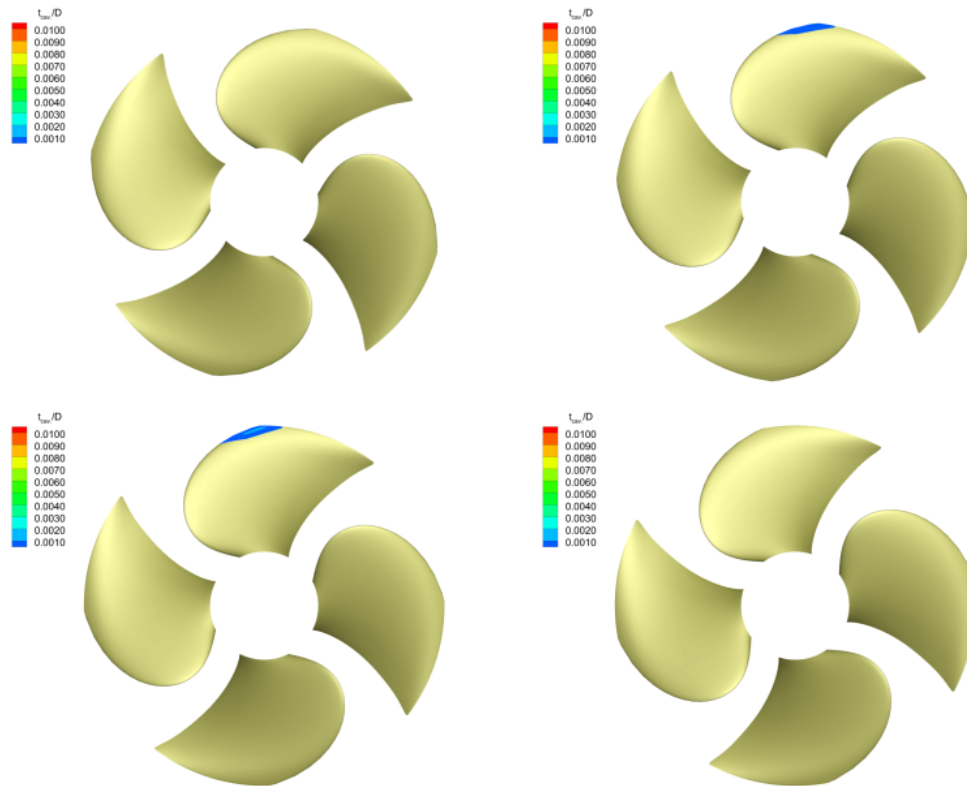


Figure 9: Predicted cavity extension (BEM) with Nominal inflow wake.

and chordwise direction) exists when the Nominal wake is adopted in the BEM calculations. The use of the Nominal wake or of the Nominal – LDV wake has not a marked effect on the predictions, as shown in Figure 10. On the contrary, the use of the Effective wake (see Figure 11) results in a larger cavitation extent. In addition, in any case the tip vortex is not predicted, since its evaluation is beyond the capability of the adopted code. For what regards the sheet cavitation extent, some further considerations may arise. First of all, it is well-known that the BEM code has not the capability of modifying the inflow wake from the nominal to the effective one; as a consequence, in order to have a better reproduction of the behind hull behaviour of the propeller, the effective wake has to be used in BEM calculations. On the contrary, for what regards cavitation tunnel measurements, ITTC procedures prescribe to reproduce the nominal wake, implicitly considering that the interaction between the reproduced wake and the propeller results in the effective wake. However, at least in this case, the cavitation extent at cavitation tunnel is more similar to the one predicted by BEM in the nominal wake, suggesting that the propeller effect is less than expected at cavitation tunnel or, alternatively, that the coupled BEM/RANSE approach may excessively alter the effective wake. From

the cavitation tunnel point of view, this may be due to the adoption of wake screens, which represent only partially the propeller inflow due to the hull (with particular attention on the propeller disk and not on the complete wake); moreover, the hull-propeller interactions are not the same with the wake screen and with the complete hull. For what regards the numerical calculations, the coupled procedure may suffer from an over-prediction of the BEM propeller induced velocities.

For what regards pressure pulses, different analyses have been carried out. At first, the predicted values of the pressure pulses at the point for which measurements have been carried out in model scale are compared, by using as input to the propeller the three different wakes. In all cases, pressures on the flat plate resembling the tunnel configuration are considered.

The results, in terms of blade harmonics (considering from the 1st to the 4th harmonic), are reported in Figure 12.

As it can be seen, a strong difference is evidenced between the nominal and effective wake, consistently with the different cavitation extent shown in Figure 11. On the contrary, the effect of the difference between the Nominal and the Nominal - LDV wake is very limited, as already observed in the case of the cavitation. From this point of

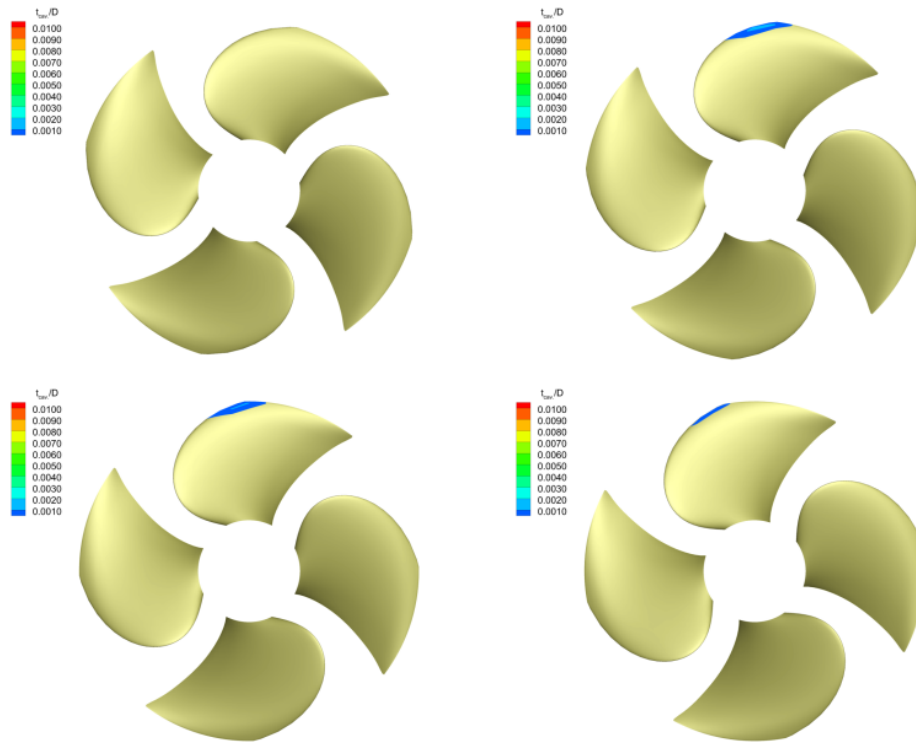


Figure 10: Predicted cavity extension (BEM) with Nominal-LDV inflow wake.

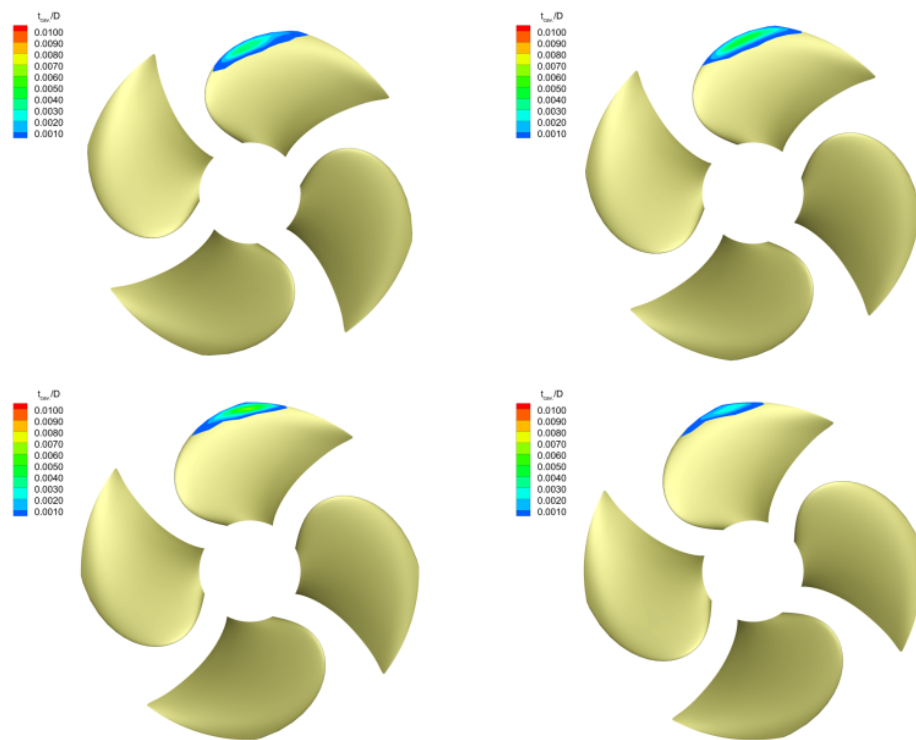


Figure 11: Predicted cavity extension (BEM) with Effective inflow wake.

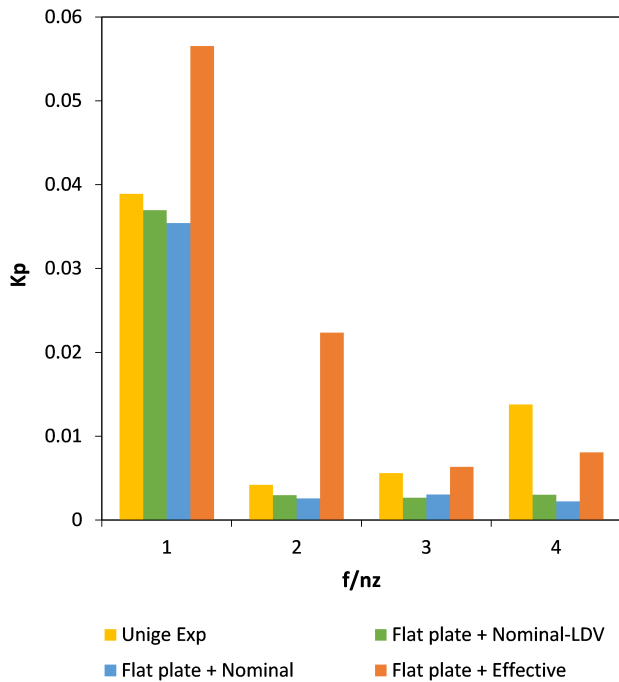


Figure 12: Pressure pulses in correspondence to the cavitation tunnel measuring point. Comparison between numerical results (different inflow wakes) and experimental measurements.

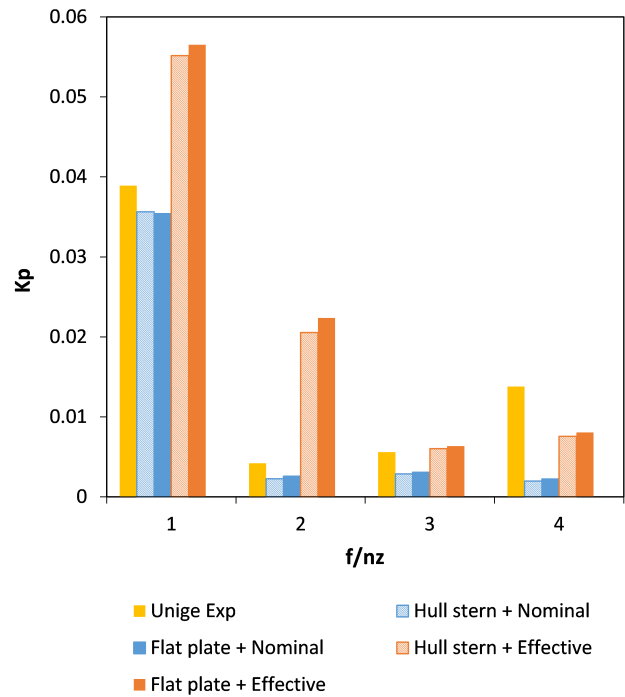


Figure 13: Pressure pulses in correspondence to the cavitation tunnel measuring point. Effect of hull shape and inflow wakes.

view, it may be underlined that the most significant differences between the two wakes are localised at lower radii, thus not affecting neither cavitation nor the resultant pressure pulses, which are, instead, more influenced by the propeller behaviour at the outer radii. For what regards the pressure pulses values, the predictions using the nominal wake are in fair agreement with the experimental results. On the contrary, the values obtained with the effective wake are much larger, considering especially the first and second harmonic. In this case it has to be remarked that, from previous analyses, it appeared that BEM codes tend to overestimate the effect of sheet cavitation on pressure pulses, as reported in [32]. Only in the case of the fourth harmonic values computed considering the effective wake are more in line with experimental results. Since the fourth harmonic in the experimental results is likely to be related to the cavitating tip vortex, which is not considered in the BEM calculations, this correspondence may not be ascribed to a better reliability of the calculations with the effective wake.

As a second step, the possible effect of the adoption of the real hull shape or the flat plate has been investigated by comparing the numerical results in correspondence to both the nominal and the effective wake (the Nominal – LDV wake has not been considered for these calculations). As it can be seen from the results reported in Figure 13,

the influence is very limited and definitely much lower than the effect of the use of the nominal or the effective wake. This is partially due to the fact that the point analyzed, being above the propeller disk, has the same distance and the local hull curvature is similar in the two cases, while the hull shape varies from the flat plate only when moving sideward. However, also considering different points (namely points at different lateral positions as those used during the sea trials), the result is qualitatively similar, with very small differences between the two cases, as reported in Figure 14, where the first harmonic non-dimensional amplitudes ($K_p = \frac{2p}{\rho N^2 D^2}$) at different lateral positions are reported.

As a final step of this analysis, the full-scale measurements have been compared with the numerical prediction and with model scale results.

Before presenting this comparison, it is worth mentioning that, as showed in the previously paragraph, the full scale measurements have been performed at a slightly different longitudinal position (shifted by about 0.1 R towards the bow) with respect to the one considered in model tests, in which the sensor was located exactly above the propeller tip.

In order to analyse the possible influence of this difference, numerical calculations have been carried out in correspondence of points placed at three different longitu-

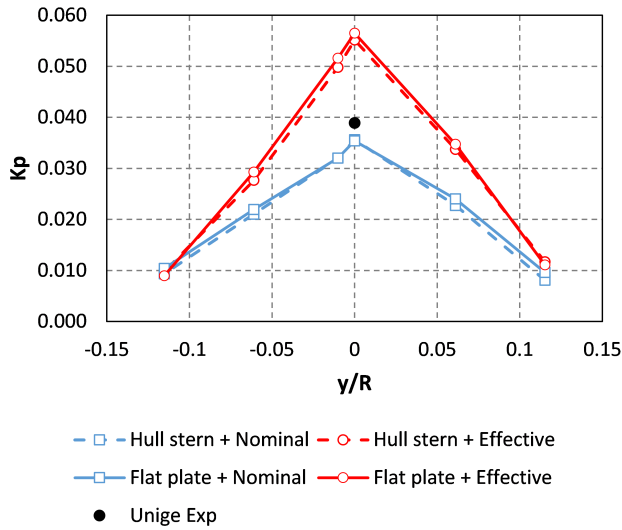


Figure 14: First harmonic values in correspondence to different transversal points at longitudinal propeller plane position. Effect of the hull shape and of nominal and effective wakes.

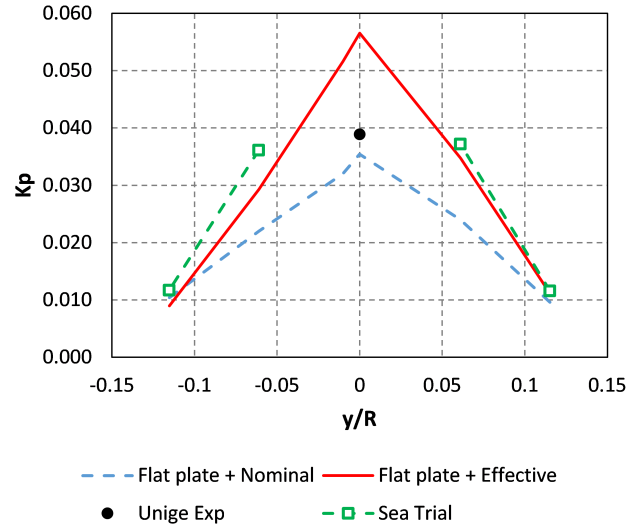


Figure 16: Comparison between predicted and measured pressure pulses (first harmonic) in cavitating condition on the transversal section in correspondence of the propeller disk.

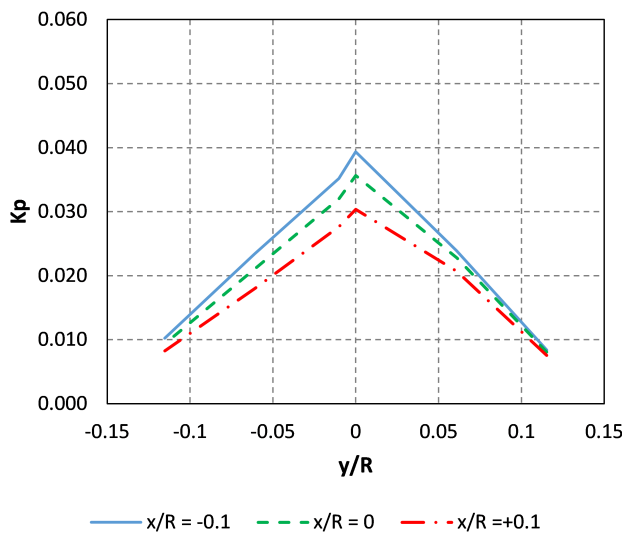


Figure 15: First harmonic values in correspondence to different points on the hull stern. Influence of the longitudinal position with the full-scale Nominal inflow wake.

dinal positions (*i.e.* at propeller disk and shifted by 0.1 R aft and fore). The results of this analysis are reported in Figure 15 in terms of first blade harmonics; in the figure, a positive value of the longitudinal position corresponds to a shift towards stern, consistently with the reference frame adopted in the BEM calculations.

The effect of a shift towards bow results in a slight (but evident) increase of the harmonic values, which has to be considered when the two experimental results are compared; in particular, an increase by about 10% is present when shifting forward.

The numerical results and the model tests measurements have been compared with the full-scale measurements in Figure 16. In this case, numerical results considered are those obtained with the complete hull stern shape, with the Nominal and the Effective in full scale. Unfortunately, as anticipated before, full scale trials results are not available for the position above the propeller tip, since the correspondent pressure sensor had a failure during tests. Full-scale measurements, where available, are however in very good agreement with those obtained numerically when the effective wake is considered. These numerical results (at least the tendency) might be thus adopted in correspondence of the mid-point in order to complete the values of the experimental results.

A significant difference may clearly be evidenced between the results, with an underestimation of the pressure pulses in full scale when considering the nominal wake field.

These conclusions, however, have to be considered carefully, because they are affected by some uncertainties. In particular, as already mentioned, the reliability of BEM calculations tends to be lower when cavitating conditions with a larger extent of sheet cavitation are present, leading to an overestimation of pressure pulses, especially in terms of first harmonic amplitude. This, therefore, might mask some other effect, such as possible uncertainties in the full-scale testing conditions (*e.g.* the effective pitch of the propeller, etc.). Similar considerations apply in the case of the second, third and fourth pressure pulse harmonics, shown for completeness in Appendix A. Trends

are similar also for high order harmonics (especially for the second), even if with some differences. In particular, model test results show higher values in correspondence to third and fourth harmonics, being the third in line with the calculated values with the effective wake and the fourth even higher than the calculations in the same inflow condition. The positive correlation between full scale measurements and calculations performed with the effective wake is confirmed, even if unfortunately no data about the fourth harmonic is available and, in general, the same considerations about the reliability of the results discussed for the first apply also to higher order harmonics.

Further analyses are needed, therefore, for a better understanding of this problem. This should involve, from the experimental point of view, a comparison of measurements with different facilities, allowing to analyse the influence of the use of wake screen instead of the complete hull model. Such an analysis has been carried out recently [33], showing a rather limited effect of the experimental setup, even if the nominal wake was considered in the wake screen representation. However, unfortunately a different hull form was involved, precluding any conclusion. It would be also beneficial to perform measurements of the nominal wake and of the total wake in front of the propeller, in order to indirectly derive the influence of the effective wake on the propeller performance.

In parallel, from a numerical point of view further calculations with the higher fidelity viscous codes would allow to reduce the uncertainties currently highlighted and reasonably ascribed to the adoption of BEM calculations, which, as mentioned, may result in an overestimation of the pressure pulses.

5.2 Radiated noise

5.2.1 Model-scale cavitation noise

One of the main concerns when dealing with noise tests at cavitation tunnels is the signal to noise ratio. As already remarked in Section 4.1 the background noise correction is applied to noise ratio as a part of the whole post processing procedure. However, before doing this, it could be useful to analyze directly noise levels received at the hydrophones, reported in Figure 17 and Figure 18.

As it can be seen the signal to noise ratio is rather good for both hydrophones for frequencies above 200 Hz, especially if attention is focused on the continuous part of the spectra.

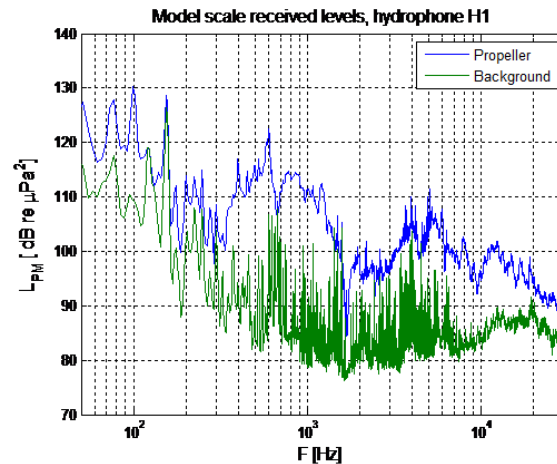


Figure 17: Cavitation tunnel received levels, hydrophone H1.

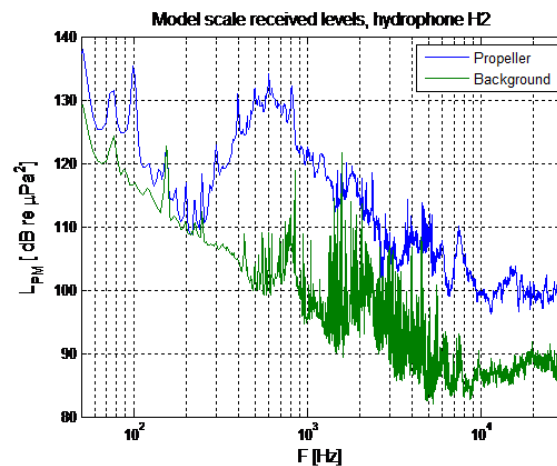


Figure 18: Cavitation tunnel received levels, hydrophone H2.

Moreover, the spectra of the two sensors are rather different, mainly because of differences in the noise propagation. Actually, due to its particular position, noise spectra measured by hydrophone H1 (placed in the external tank) are significantly different with respect to those measured by H2 (directly inside the tunnel) which are, however, still affected by the effects of the confined environment.

This phenomenon is one of the well-known problems related to propeller radiated noise measurements in model scale. In particular, the presence of tunnel walls or the particular location of hydrophones, as H1 in present case, may affect significantly the measurements. Therefore, it is recommended by ITTC [34] to evaluate this effect and to correct measurements before performing full-scale predictions.

Transfer functions have been evaluated following the procedure described in [35] for the frequency range 500:30000 Hz according to the transmitting capability of

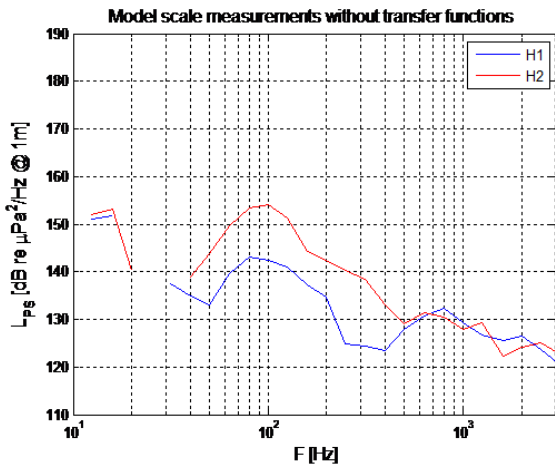


Figure 19: Cavitation tunnel noise prediction without considering transfer functions.

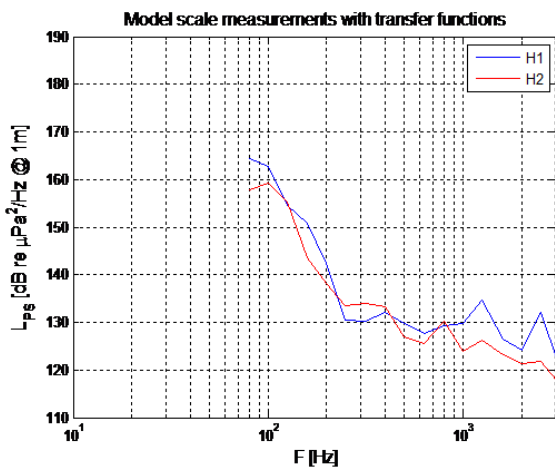


Figure 20: Cavitation tunnel noise prediction considering transfer functions.

the transducer. This frequency range when scaled to full-scale corresponds to about 80:4500 Hz.

The effect of the transfer functions is evidenced in Figure 19 and Figure 20.

In the second figure the same predictions are evaluated considering also the confined environment effect by means of the measured transfer functions.

In these cases, one third octave band representation is adopted for clarity. The first figure reports the full-scale predictions computed for the two hydrophones without considering the transfer functions. Only those portions of the spectra with signal to noise ratio higher than 3 dB are reported.

The transfer functions correction results in almost eliminating the differences between measurements from the two hydrophones with different configurations, de-

scribed in §4.1, despite being such differences initially remarkable.

The fact that spectra obtained considering transfer functions are shown only for frequencies higher than 80 Hz in full scale is due to the already mentioned frequency range for which transfer functions were evaluated.

Thanks to the good agreement between the two hydrophones after the correction, the final full-scale prediction may be done computing the average of the spectra from the two sensors.

5.2.2 Full-scale radiated noise

Full-scale noise data have been collected following the procedure described in §4.2 providing useful information for the study of ship noise and the validation of model scale experimental procedures.

Raw data consist of noise records from the hydrophones lasting the time of the complete ship passage near the buoy.

With the aim of characterising the underwater noise emission of the ship, only a part of the signal around the CPA (see [27]) is taken into account. This part of signal is analysed in detail. In Figure 21, the 1/3 octaves band levels and the narrow band spectrum for the considered case are reported. The results shown in Figure 21 are referred to the standard distance of one metre from the source using for the transmission losses the $20\log(R)$ correction factor. Even if it would be more accurate to numerically evaluate the actual transmission losses, this is in line with the prescriptions of [27] and it has the advantage of simplifying possible comparisons and re-use of the data.

As it can be noted in the figure, the spectrum has the typical shape of the ship underwater noise with more energy concentrated at the lower frequencies and a linear (in logarithmic scale) decay at higher frequencies.

Full-scale measurements give a picture of the total noise emission of the ship. The overall noise emission is the result of the superimposition of the contribution of many different sources: propeller, machinery and flow around the hull. Flow noise is important for high speed, therefore for the present case it has a very low influence as the ship was sailing at 12 knots. The cavitating propeller noise represents the major contribution and it is responsible for the broadband noise on the entire frequency range. A detailed analysis of the main contributions can be performed by making reference to Figure 22. The noise generated by the propeller presents two main components: tonal components linked to the blade passing frequency and broadband noise with characteristics depending on the

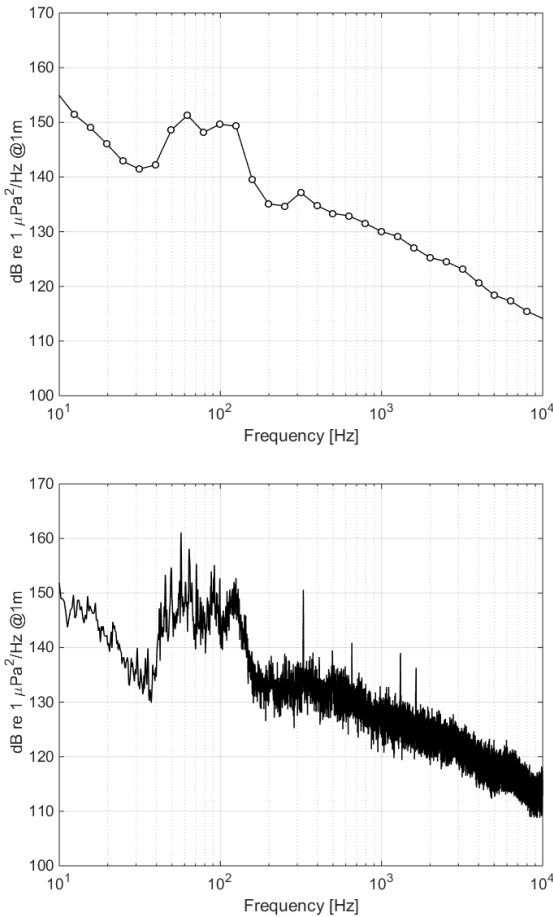


Figure 21: 1/3 octaves band levels (upper figure) and Narrow band spectrum (lower figure) for the underwater noise emitted by the vessel.

cavitation type occurring on the propeller. The frequencies of the tonal components linked to engines and propellers can be found by simple calculations. Aim of this analysis is to distinguish, in the full-scale measurements, the contribution to the overall noise due to engines from the contribution coming from the propeller.

As regards the propeller, the blade passing frequency (BPF) and its higher harmonics are defined as:

$$BPF = \frac{RPM_P}{60} \cdot Z \cdot h, \quad h = 1, 2, \dots, H \quad (1)$$

where RPM_P are the blade revolutions per minute and Z is the number of propeller blades.

As regards the machinery, the cylinder firing rate (CFR) and its harmonics are linked to the single cylinder firing occurring every two revolutions of the engine crank for four stroke engines. They are defined as follows:

$$CFR = \frac{RPM_E}{120} \cdot h, \quad h = 1, 2, \dots, H \quad (2)$$

where RPM_E are the engine revolutions per minute.

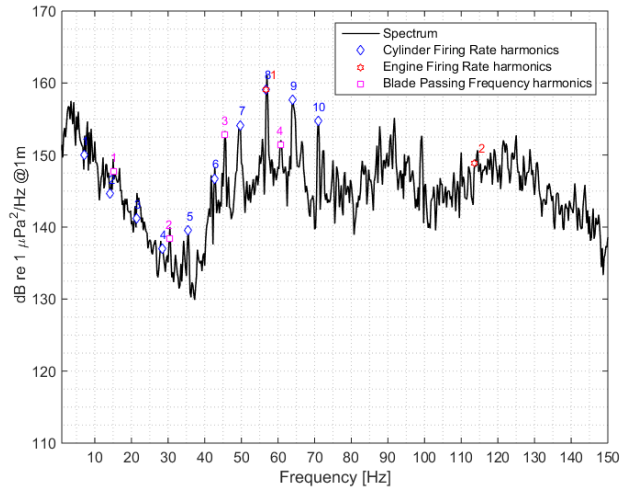


Figure 22: Enlargement of Figure 21 in the band 1–140 Hz with engine and propeller tonal components highlighted.

As many cylinders are present in the engine an engine firing rate (EFR) and its higher harmonics can be identified as:

$$EFR = CFR \cdot N \cdot h, \quad h = 1, 2, \dots, H \quad (3)$$

where N is the number of cylinders.

Looking at Figure 22 it can be seen that the engine tones can be clearly identified up to 70 Hz. In such low frequency range, the contribution coming from the propeller is responsible for the broadband floor-level from which the tonal components emerge. At higher frequencies cavitation noise is the main contribution. In particular, the hump located in the 40–140 Hz band (see also Figure 21) is typical for tip vortex cavitation.

5.2.3 Comparison Full-scale model-scale

In order to make a comparison between full scale and model scale noise measurements, several aspects must be taken into account and both measurements should be corrected in order to represent the ideal free field radiated noise. Noise spectra measured at cavitation tunnel have been already scaled to full scale and corrected for the confined environment effect as previously explained. As regards the full scale measurements, transmission losses have been evaluated numerically using a wave-number integration algorithm for frequencies below 1 kHz and a ray-tracing algorithm for frequencies higher than 1 kHz. Such propagation models has been chosen as they are both physically and practically applicable, in the specific frequency range above mentioned, for a shallow water range independent case [36]. Both algorithms require in input

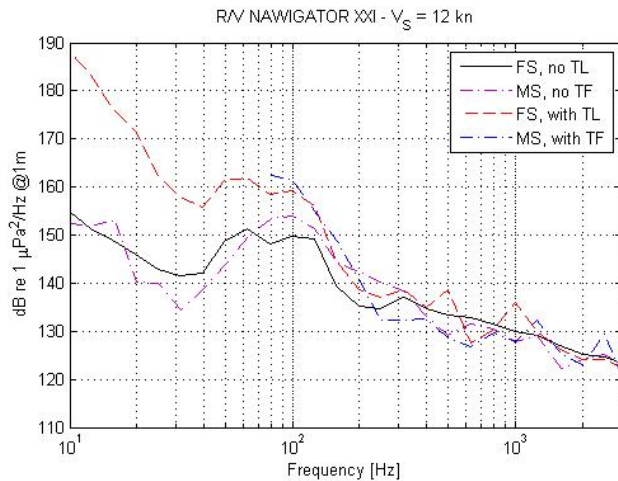


Figure 23: Comparison between full scale underwater noise and model scale propeller noise measurements – application of transfer function in model scale and transmission losses in full scale.

the environmental characteristic of the specific test situation such as sound speed in the water column, bathymetry and bottom composition. The celerity profile in the water column was measured during the trial as well as the sea depth. The distance between the ship and the hydrophones was around a hundred meters and therefore the bottom was considered flat. As regards the sea bottom characteristics, thickness and composition of the sediment were not directly monitored, therefore they were derived by databases. The sediment thickness was taken from [37], which provides information on a grid of points on the ocean bottoms with a resolution of one minute. The composition of the sediment was derived from the Deck41 database, where ten different kinds of sediments are present.

As it can be seen looking at Figure 23, the influence of the two corrections is quite evident, particularly at low frequency.

Further, the two modified curves (red curve for full-scale measurements considering transmission loss, blue curve for predictions from model scale including transfer function) appear very similar, reducing the initial discrepancies and increasing in both cases the maximum noise levels. It has to be remarked that the very good correspondence of these two curves is not to be considered as a standard: usually, discrepancies of about 5 – 10 dB may be expected.

6 Conclusions

The paper provides an up-to-date picture of the procedures that can be applied for the prediction of side effects of propeller cavitation in terms of pressure pulses and radiated noise. A test case, represented by a single screw research vessel for which experimental results in model and full scale were available, has been considered, analyzing the capability of numerical tools and the reliability of model scale tests in a small size cavitation tunnel.

For what regards pressure pulses, the importance of the correct representation of the ship wake in full scale has been confirmed. This includes, both for model tests and numerical calculations, not only the nominal wake but also the effect of the interaction between the hull and the propeller. From this point of view, possible problems may arise in model tests in case the nominal wake is represented by means of wake screens, since their interaction with the propeller is different from the one between the propeller and the hull. From a numerical point of view, the proposed coupled BEM/RANSE approach may suffer from discrepancies in the evaluation of the propeller induced velocities, which in turn affect the predicted effective wake. Moreover, BEM codes tend to overestimate the effect of cavitation, when its extension becomes large, on induced pressures. Further analyses are needed, in future, comparing, in model scale, results among different facilities where complete hull forms can be employed or where wake screens are adopted. In parallel, the prediction of pressure pulses by means of a full RANSE approach should be considered, assessing the merits (in terms of higher fidelity) and the shortcomings (in terms of higher computational demand) of such approach.

For what regards the radiated noise, activities have been limited only to the experimental part, having considered the direct numerical prediction of radiated noise as a still too demanding issue. Even limiting to this, many problems arise, related to the scale effect on cavitation mechanisms and consequently on radiated noise and, in general, to confined environment of model testing facilities. Also in full-scale, the environment effect may play a significant role, thus leading to the necessity of suitable methods to account for it. The proposed approaches are promising, allowing obtaining for the present test case a remarkably good correspondence between full-scale measurements and predictions from model tests. However, more data are needed in future to gain further confidence on the procedures and on the complex mechanisms of cavitating propeller noise generation.

Acknowledgement: This work was developed in the frame of the collaborative project AQUO (Achieve Quieter Oceans by shipping noise footprint reduction), funded by the European Commission within the Call FP7 SST.2012.1.1-1: Assessment and mitigation of noise impacts of the maritime transport on the marine environment, Grant agreement no 314227, coordinated topic “The Ocean of Tomorrow”. The content of this paper does not reflect the official opinion of the European Union. Responsibility for the information and views expressed in the paper lies entirely with the authors.

References

- [1] IMO 1991 Assembly Resolution A.719 (17) on Prevention of Air Pollution from Ships.
- [2] IMO 2014 Guidelines for the reduction of underwater noise from commercial shipping to address adverse impacts on marine life MEPC.1/Circ.833 7 April 2014
- [3] SILENV (Ships oriented innovative solutions to reduce noise and vibrations) European Commission within the Call FP7 <http://www.silenv.eu/>
- [4] SONIC (Suppression Of underwater Noise Induced by Cavitation) European Commission within the Call FP7 <http://www.sonic-project.eu/>
- [5] AQUO (Achieve Quieter Oceans by shipping noise footprint reduction) European Commission within the Call FP7 <http://www.aquo.eu/>
- [6] K. Wöckner, M. Greve, M. Scharf, M. Abdel-Maksoud and T. Rung, “Unsteady Viscous/Inviscid Coupling Approaches for Propeller-Flow Simulations”, Proceedings of the Second Symposium on marine propulsors, SMP2011, Hamburg, Germany, 2011.
- [7] D. Villa, S. Gaggero and S. Brizzolara, “Ship Self Propulsion with different CFD methods: from actuator disk to viscous inviscid unsteady coupled solvers”, Proceedings of the 10th International Conference on Hydrodynamics, ICHD2012, St. Petersburg, Russia, October 2012.
- [8] S. Berger, M. Bauer, M. Druckenbrod, M. Abdel-Maksoud “An efficient viscous/inviscid coupling method for the prognostic of propeller –induced hull pressure fluctuations” Proceeding of 17th International Conference on Ship and Shipping Research NAV2012, Naples Italy, 17-19 October 2012 ISBN: 979-88-904394-4-5 (eBook) 979-88-904394-2-1.
- [9] Gaggero S., Gonzalez-Adalid J.G. and Perez Sobrino M., “Design of Contracted and Tip Loaded Propellers by using Boundary Element Methods and Optimization Algorithms”, Applied Ocean Research, Volume 55, February 2016, pp. 102–129, ISSN:0141-1187, DOI:10.1016/j.apor.2015.12.004.
- [10] D.Q. Li, J. Hallander, T. Johansson and R. Karlsson, “Cavitation dynamics and underwater radiated noise signature of a ship with cavitating propeller”, Proceedings of the VI International Conference on Computational Methods in Marine Engineering, MARINE2015, Rome Italy, 2015.
- [11] D.Q. Li, J. Hallander, T. Johansson, “Towards numerical prediction of pressure pulses and underwater radiated”, Fourth International Symposium on Marine Propulsors, SMP 2015, Austin, Texas, USA, 2015
- [12] T. Bugalski and P. Hoffmann, “Numerical Simulation of the Self-Propulsion Model tests”, Proceedings of the Second international Symposium on Marine Propulsors, SMP2011, Hamburg, Germany, 2011.
- [13] M. Greve, K. Wöckner-Kluwe, M. Abdel-Maksoud, and T. Rung, “Viscous-Inviscid Coupling Methods for Advanced Marine Propeller Applications”, Hindawi Publishing Corporation, International Journal of Rotating Machinery, Volume 2012, Article ID 743060, 12 pages doi:10.1155/2012/743060
- [14] D. Villa, S. Gaggero, S. Brizzolara, “Simulation of ship in self propulsion with different CFD methods: From actuator disk to potential flow/RANS coupled solvers”, RINA, Royal Institution of Naval Architects - Developments in Marine CFD, pp. 1-12. 2011.
- [15] C.Y. Hsin, “Development and analysis of Panel methods for Propellers in Unsteady Flow”, Ph.D. Thesis, Department of Ocean Engineering, 1990.
- [16] N.E. Fine, “Nonlinear Analysis of Cavitating Propellers in Nonuniform flow”, Ph.D. Thesis, department of Ocean Engineering, 1992.
- [17] S. Gaggero, D. Villa, S. Brizzolara, “RANS and Panel Methods for Unsteady Flow Propeller Analysis”, Journal of Hydrodynamics, Ser. B, Volume 22, Issue 5, Supplement 1, 10-15 October 2010, p. 564-569 (547-552), ISSN: 1001-6058
- [18] S. Gaggero, D. Villa, M. Viviani, “An investigation on the discrepancies between RANSE and BEM approaches for the prediction of marine propeller unsteady performances in strongly non-homogeneous wakes”, Proceedings of the International Conference on Offshore Mechanics and Arctic Engineering - OMAE, 2014, DOI: 10.1115/OMAE2014-23831
- [19] D. Bertetta, S. Brizzolara, E. Canepa, S. Gaggero and M. Viviani, “EFD and CFD characterization of a CLT propeller”, International Journal of Rotating Machinery, Volume 2012, Article ID 348939, p.1-23, ISSN: 1023-621X (Print), ISSN: 1542-3034 (Online), DOI:10.1155/2012/348939.
- [20] ITTC Recommended Procedures and Guidelines (2014) “Model scale noise measurements – 7.5–02–01–05”
- [21] ITTC The Specialist Committee on Water Quality and Cavitation. Final report and recommendations to the 23rd ITTC, Proceedings of the 23rd (ITTC) International Towing Tank Conference, Venice, Italy, 2002.
- [22] ITTC Specialist Committee on Hydrodynamic Noise , “Final Report and Recommendations to the 27th ITTC”, September 2014, Copenhagen
- [23] G. Tani, M. Viviani, E. Armelloni, M. Nataletti, “Cavitation Tunnel Acoustic Characterisation and Application to Model Propeller Radiated Noise Measurements at Different Functioning Conditions”, Proceedings of the Institution of Mechanical Engineers, Part M: Journal of Engineering for the Maritime Environment; (2015) ISSN: 1475-0902, SAGE Publishings, p.1-17, doi: 10.1177/1475090214563860
- [24] M. André, T. Gaggero, E. Rizzuto, “Underwater noise emissions: Another challenge for ship design”, Advances in Marine Structures - Proceedings of the 3rd International Conference on Marine Structures, MARSTRUCT 2011, (2011) pp. 581-591.
- [25] T. Gaggero, M. Van Der Schaar, R. Salinas, P. Beltrán, E. Rizzuto, M. André, “Uncertainties in measurements of ship underwater noise emissions”, 11th European Conference on Underwa-

- ter Acoustics 2012, ECUA 2012, 34 2 (PART 3), pp. 1876–1885.
- [26] A. Badino, D. Borelli, T. Gaggero, E. Rizzuto and C. Schenone, “Normative framework for ship noise: Present situation and future trends”, *Noise Control Engineering Journal*, 60 (6), (2012), pp. 740-762. DOI: 10.3397/1.3701045
- [27] ANSI/ASA, 2009. ANSI /ASA S12.64-2009/Part 1. Quantities and Procedures for Description and Measurement of Underwater Sound from Ships - Part 1: General Requirements. Acoustical Society of America.
- [28] T. Gaggero, M. van der Schaar, R. Salinas, P. Beltrán, E. Rizzuto, M. André, “Directivity Patterns of Ship Underwater Noise Emissions”, In: *Proceedings of the 1st Underwater Acoustics Conference and Exhibition*. Athens : pp. 1295- 1301, (2013), Corfù (GR), ISBN: 9786188072503
- [29] T. Gaggero, M. Bassetti, E. Firenze, A. Tesei, A. Trucco, “Processing strategies for evaluating the ship radiated noise using an underwater vertical array”, in *Proceedings of the 2nd Underwater Acoustics Conference and Exhibition 23-27 (2014)*, Rodi, Greece.
- [30] Rijpkema, D., Starke, B. and Bosschers, J. (2013), Numerical simulation of propeller-hull interaction and determination of the effective wake field using a hybrid RANS-BEM approach, in ‘*Proceedings of the 3rd International Symposium on Marine Propulsors*’, 5th-7th May, Launceston.
- [31] S. Gaggero, D. Villa, M. Viviani, “An extensive analysis of numerical ship self-propulsion prediction via a coupled BEM/RANS approach. Part I: the KCS test case. Under review on *Applied Ocean Research*.
- [32] *Proceedings of the Second Workshop on Cavitation and Propeller Performance - The Fourth International Symposium on Marine Propulsors*, Edited by: S. Kinnas, M. Abdel-Maksoud, U. Barkmann, L. Lübke, Y. Tian, ISBN: 978-0-9964594-4-0
- [33] AQUO (Achieve QUIeter Oceans by shipping noise footprint reduction), WP 2: Noise sources, Deliverable 2.5: Experimental investigations in model scale - Propeller noise experiments in model scale
- [34] H. Sasajima, I. Tanaka, “On the estimation of wakes of ships”. *Proceedings of the 11th (ITTC) International Towing Tank Conference*, Tokyo, (1966).
- [35] E. Rizzuto, G. Tani, M. Viviani, “Experimental Analysis of the Influence of Ship Wake Scaling on Marine Propeller Radiated Noise and Pressure Pulses”, *Proceedings of The 21st International Congress on Sound and Vibration (ICSV 2014)*, Beijing, 13-17 July 2014 - invited lecture, p. 1–8, Editor: Acoustical Society of China (ASC), International Institute of Acoustics and Vibrations, (2014) ISBN: 978-83-62652-66-2, ISSN: 2329-3675
- [36] Etter, P., “*Underwater Acoustic Modeling and Simulation*”. Spon Press, 2003
- [37] D.L Divins, “*Total Sediment Thickness of the World’s Oceans & Marginal Seas*”, NOAA National Geophysical Data Center, Boulder, CO, 2003.

Appendix A

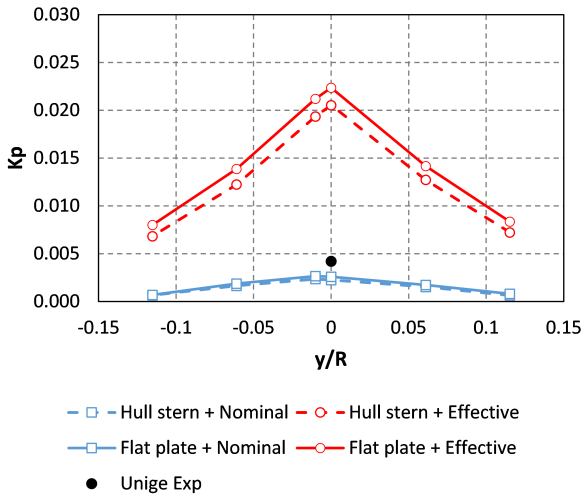


Figure A.1: Effect of the hull shape and of nominal and effective wakes in correspondence of different transversal point at longitudinal propeller plane position. Second harmonic values.

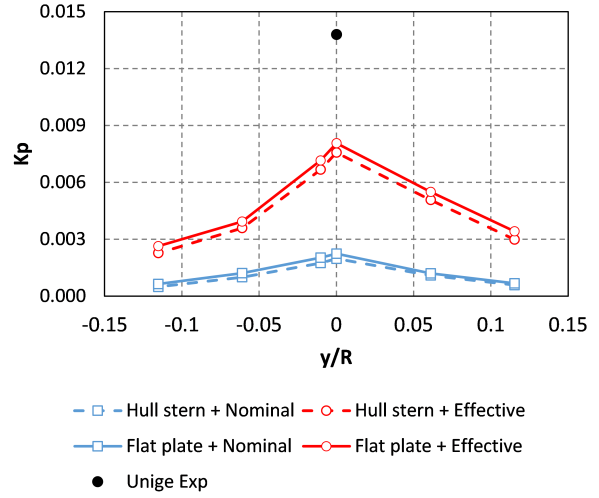


Figure A.3: Effect of the hull shape and of nominal and effective wakes in correspondence of different transversal point at longitudinal propeller plane position. Fourth harmonic values.

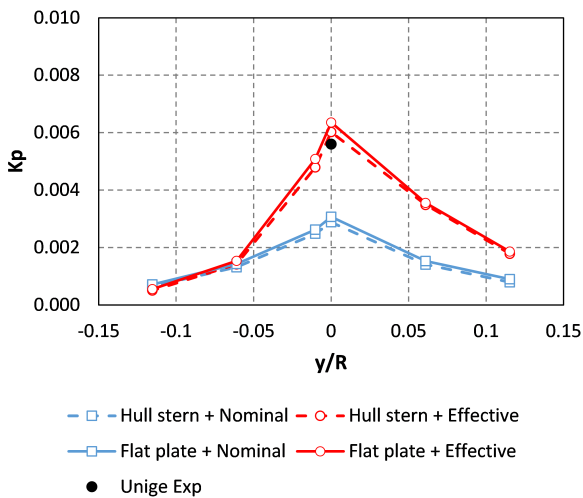


Figure A.2: Effect of the hull shape and of nominal and effective wakes in correspondence of different transversal point at longitudinal propeller plane position. Third harmonic values.

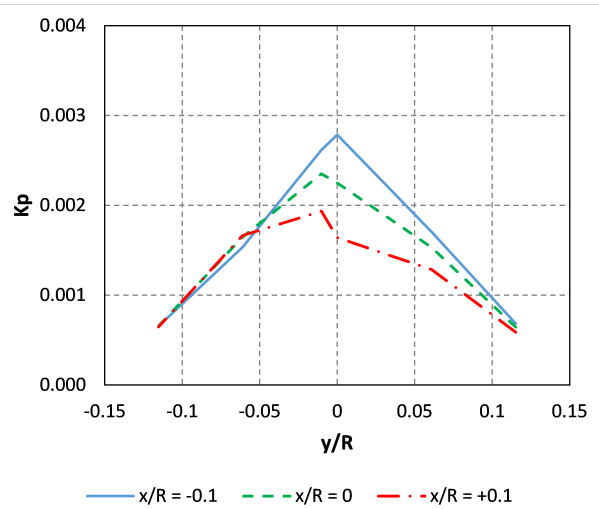


Figure A.4: Second harmonic values in correspondence to different points on the hull stern. Influence of the longitudinal position with the full-scale Nominal inflow wake.

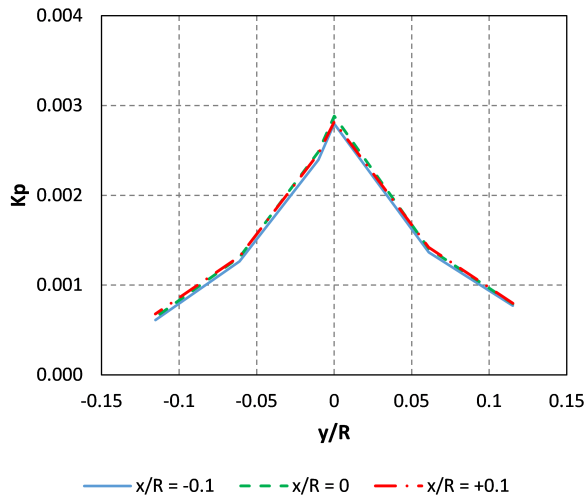


Figure A.5: Third harmonic values in correspondence to different points on the hull stern. Influence of the longitudinal position with the full-scale Nominal inflow wake.

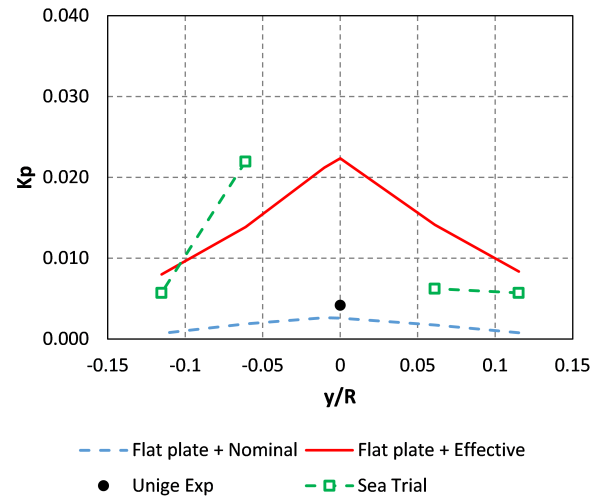


Figure A.7: Comparison between predicted and measured pressure pulses (second harmonic) in cavitating condition on the transversal section in correspondence of the propeller disk.

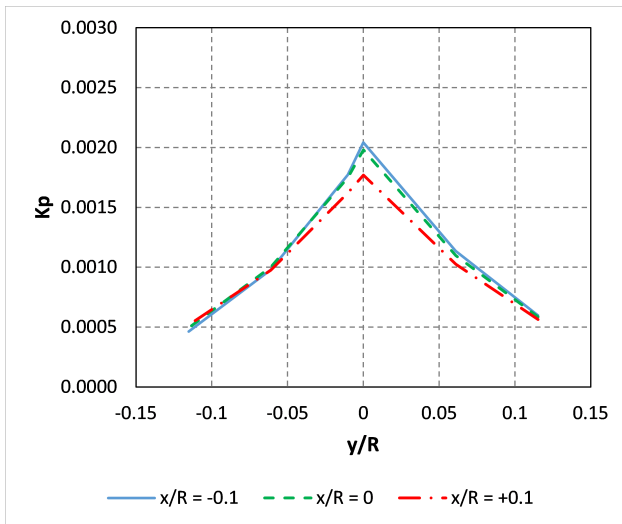


Figure A.6: Fourth harmonic values in correspondence to different points on the hull stern. Influence of the longitudinal position with the full-scale Nominal inflow wake.

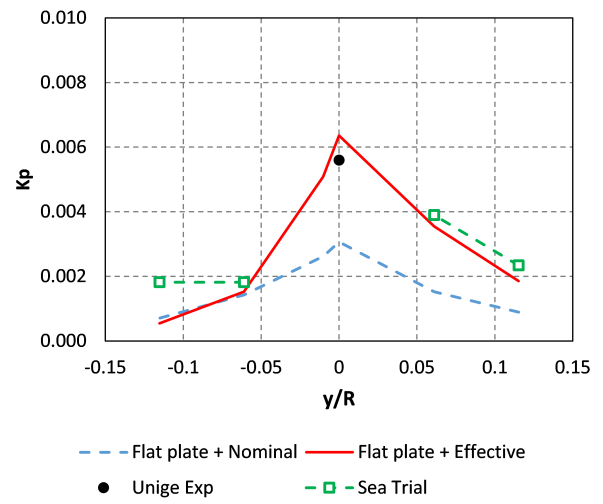


Figure A.8: Comparison between predicted and measured pressure pulses (third harmonic) in cavitating condition on the transversal section in correspondence of the propeller disk.

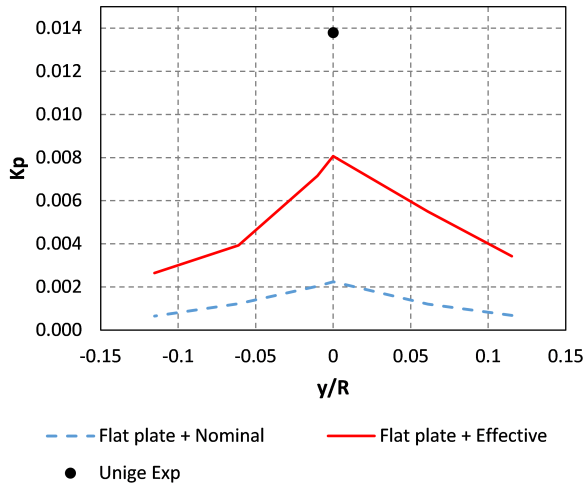


Figure A.9: Comparison between predicted and measured pressure pulses (fourth harmonic) in cavitating condition on the transversal section in correspondence of the propeller disk. (no full-scale measurements available)